Contemporary Mathematics
https://ojs.wiserpub.com/index.php/CM/

Research Article

Directed Transport of a Short Polymer Chain on a Temperature-Dependent Ratchet Potential

Mesfin Asfaw Taye

Science Division, West Los Angeles College, 9000 Overland Ave, Culver City, CA, 90230, USA
E-mail: tayem@wlac.edu

Received: 27 February 2025; **Revised:** 15 April 2025; **Accepted:** 24 April 2025

Abstract: We investigate the transport properties of a single flexible polymer chain moving along a periodic ratchet potential modulated by a spatially varying temperature. At steady state, the polymer exhibits rapid unidirectional motion, with the efficiency of current rectification strongly influenced by its elasticity and size. Analytical and numerical analyses demonstrate that the steady-state transport can be effectively regulated by modulating the elastic constant. Notably, the stall force, at which the polymer current ceases, remains independent of both chain length and coupling strength. Beyond the stall force, the polymer's mobility exhibits a strong dependence on its flexibility and size. These results highlight a tunable mechanism for controlling polymer transport, offering potential applications in directed polymer motion and the sorting of multicomponent systems based on intrinsic material properties.

***Keywords*:** polymer transport, ratchet potential, temperature gradient, stochastic dynamics, elastic coupling

MSC: 82C31, 82D60

1. Introduction

The transport dynamics of biological systems, such as polymers and membranes, have garnered significant interest due to their intrinsic complexity and the influence of internal degrees of freedom on their motion [1–6]. These systems often consist of multiple interacting components arranged in intricate architectures, leading to transport behaviors that exhibit nontrivial dependencies on size, flexibility, and thermal background. Prior studies on polymer dynamics in bistable potentials have demonstrated that escape rates are highly sensitive to molecular size and inter-monomer interactions [7–18]. Similarly, the interplay between stochastic fluctuations and periodic forces in time-dependent potentials has been shown to induce stochastic resonance, facilitating controlled polymer transport [19–21]. Notably, recent investigations into linearly coupled polymers overcoming potential barriers have revealed that optimal resonance temperatures can lead to enhanced directional transport, with implications for biomolecular applications, including Deoxyribonucleic Acid (DNA) manipulation [7–12].

In this work, we systematically examine the rectified motion of a flexible polymer chain moving along a periodic ratchet potential coupled with a spatially varying temperature. Unlike previous studies on polymer transport in rocking or flashing ratchets [22–24], where directional transport can be modulated by tuning polymer flexibility, our approach

DOI: https://doi.org/10.37256/cm.6420256640

incorporates an external load and considers a medium in thermal contact with alternating hot and cold reservoirs along the spatial coordinate. Our numerical and analytical results reveal that the polymer exhibits a rapid unidirectional current, with rectification strength governed not only by the external load and thermal gradient but also by the polymer's coupling strength and size.

A key finding of this study is the dependence of the polymer's velocity on the coupling strength k. For finite k, the chain's mobility exhibits a peak, but as k increases further, velocity diminishes. Moreover, velocity is strictly load-dependent, decreasing with increasing external force until reaching a stall force, beyond which the polymer reverses direction and its velocity grows with load. Remarkably, our analysis demonstrates that the stall force at which the polymer current vanishes is independent of both the chain length N and the coupling strength k. Additionally, velocity exhibits an optimal value at a specific potential barrier height U_0, and as the background temperature intensity rises, the polymer undergoes accelerated unidirectional transport. These numerical findings are corroborated by exact analytical results in the limits of $k \to 0$ and $k \to \infty$. As discussed before, at steady state, the chain exhibits directed transport, with efficiency strongly influenced by its elasticity and size. This behavior reflects trends seen in the mechanical response of functionally graded and graphene-reinforced composites with internal gradients [25–28]. Our results show that transport can be tuned via stiffness modulation, while the stall force remains independent of chain length or coupling strength. These findings suggest a mechanism for passive molecular sorting, aligned with current efforts in advanced composite design.

The paper is organized as follows: In Section 2, we present the model. Section 3 discusses the role of coupling strength in polymer mobility. Section 4 examines the dependence of the globular chain's velocity on model parameters. Finally, Section 5 provides a summary and conclusion.

2. The model

We consider a flexible polymer chain of size N which undergoes a Brownian motion in a one dimensional piecewise linear bistable potential with an external load $U(x) = U_s(x) + fx$ where the ratchet potential $U_s(x)$ is described by

$$U_s(x) = \begin{cases} U_0\left(\dfrac{x}{L_0} + 1\right), & \text{if } -L_0 \le x \le 0; \\ \\ U_0\left(-\dfrac{x}{L_0} + 1\right), & \text{if } 0 \le x \le L_0. \end{cases} \tag{1}$$

Here, U_0 and $2L_0$ denote the barrier height and the width of the ratchet potential, respectively, and where f is the load. The potential has a potential maxima U_0 at $x = 0$ and potential minima at $x = \pm L_0$. The piecewise linear potential is widely used in ratchet models due to its analytical tractability and ability to yield exact expressions for transport quantities. Despite its simplicity, it captures the essential features of the asymmetric energy landscapes responsible for directed motion. This form also reflects the sharp potential profiles found in microstructured or optically patterned environments, making it both mathematically and physically relevant.

In this work, the chain contour length is taken to be much less than the characteristic dimension of the ratchet potential $2L_0$. The ratchet potential is also coupled with a spatially varying temperature

$$T(x) = \begin{cases} T_h, & \text{if } -L_0 \le x \le 0; \\ \\ T_c, & \text{if } 0 \le x \le L_0 \end{cases} \tag{2}$$

as shown in Figure 1. $U_s(x)$ and $T(x)$ are assumed to have the same period such that $U_s(x+2L_0) = U_s(x)$ and $T(x+2L_0) = T(x)$. As a side remark, the use of periodic boundary conditions for both the potential and temperature is physically justified, as it models an extended spatially periodic environment such as patterned substrates or microchannels with repeating thermal and structural features. These conditions eliminate edge effects and enable the study of steady-state transport through a representative unit cell.

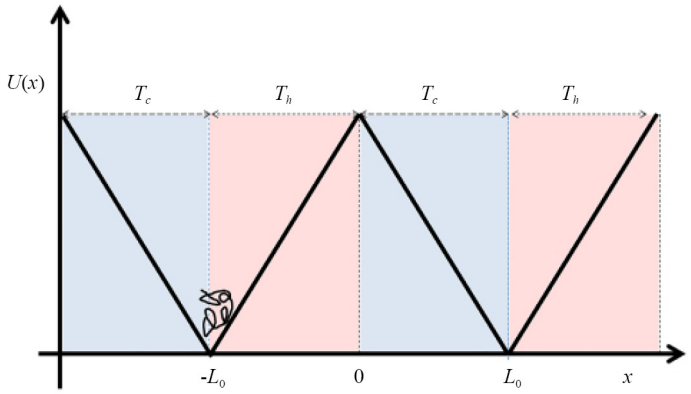

Figure 1. (Color online) Schematic diagram for initially coiled polymer chain in a piecewise linear bistable potential in the absence of an external load. The potential wells and the barrier top are located at $x = \pm L_0$ and $x = 0$, respectively. Due to the thermal background kicks, the polymer ultimately attains a steady state velocity as long as there is a distinct temperature difference between the hot and cold reservoirs

Considering only nearest-neighbor interaction between the polymer segments (the bead spring model), the Langevin equation that governs the dynamics of the N beads $(n = 1,\ 2,\ 3,\ ...,\ N)$ in a highly viscous medium under the influence of external potential $U(x)$ is given by

$$\gamma\frac{dx_n}{dt} = -k(2x_n - x_{n-1} - x_{n+1}) - \frac{\partial U(x_n)}{\partial x_n} + \sqrt{2k_B\gamma T(x_n)}\xi_n(t) \tag{3}$$

where the k is the spring (elastic) constant of the chain while γ denotes the friction coefficient. $\xi_n(t)$ is assumed to be Gaussian white noise and k_B denotes the Boltzmann constant. Hereafter, we assume k_B to be unity. At this point, we want to stress that modeling the polymer as a bead-spring chain with nearest-neighbor interactions maintains the essential elastic response and internal degrees of freedom while maintaining computational efficiency. This approach is well suited for moderately sized flexible polymers, where long-range or bending interactions are negligible. For very long chains or semiflexible polymers, higher-order effects such as bending stiffness or excluded volume may become significant, and we acknowledge these as potential extensions beyond the current model framework.

To simplify model equations we introduce a dimensionless load $\bar{f} = fL_0/T_c$, rescaled temperature $\bar{T}(x) = T(x)/T_c$, rescaled barrier height $\bar{U_0} = U_0/T_c$ and rescaled length $\bar{x} = x/L_0$. We also introduced a dimensionless coupling strength $\bar{k} = kL_0^2/T_c$, $\tau = T_h/T_c$ and time $\bar{t} = t/\beta$ where $\beta = \gamma L_0^2/T_c$ denotes the relaxation time. From now on, β and γ are taken to be unity and all the quantities are rescaled (dimensionless) so that the bars will be dropped. Experimentally, the dimensionless temperature, barrier height, and load can be determined by measuring physical quantities such as absolute temperatures, potential profiles (from optical traps), and applied forces (using optical tweezers or Atomic Force Microscopy (AFM)). This mapping enables a direct comparison between theoretical predictions and experimental conditions in colloidal or microfluidic systems.

3. Flexible polymer chain

Previous studies have shown that a single monomer (a Brownian particle) attains a directional motion when it is exposed to a ratchet potential coupled with a spatially variable temperature or an external load. For such a system, the functional dependence for the steady state current J or the velocity V on the system parameters is well explored [29–31]. However, it is not known how these results apply to a chain with several monomers. Here, we will explore the dependence of the unidirectional chain velocity as a function of key system parameters.

Next in order to understand how the velocity of the chain responds to the change to its conformational flexibility and variability that arise due to its internal degree of freedoms, we simulate the Brownian dynamics given by Equation (3) and compute the steady state current. This result is then averaged over 10^4 independent simulations. Note that in the Brownian dynamics simulations, we numerically integrate the overdamped Langevin equation, using the Euler-Maruyama method due to its efficiency and suitability for stochastic differential equations. The model is validated by comparing simulation results to exact analytical expressions in the limiting cases of $k \to 0$ and $k \to \infty$, showing excellent agreement.

To analyze further how the polymer or in general any linearly coupled system responds to the nonhomogeneous thermal noise while surmounting a double-well potential with load, the dependence of the velocity as a function of the different system parameters is explored. The numerical and analytical analyses reveal that the polymer exhibits a unidirectional current where the strength of the current rectification relies not only on the thermal background kicks and load but it has also a nontrivial dependence on its coupling strength and size. It is found that in the absence load $f = 0$, the chain maintains a positive current as long as a distinct temperature difference between the hot and cold reservoirs is retained; i.e., $T_h > T_c$, $V > 0$. For isothermal case, a one dimensional negative current can be achieved providing $f \neq 0$. In general when $T_h > T_c$ and $f \neq 0$, the polymer exhibits intriguing transport features.

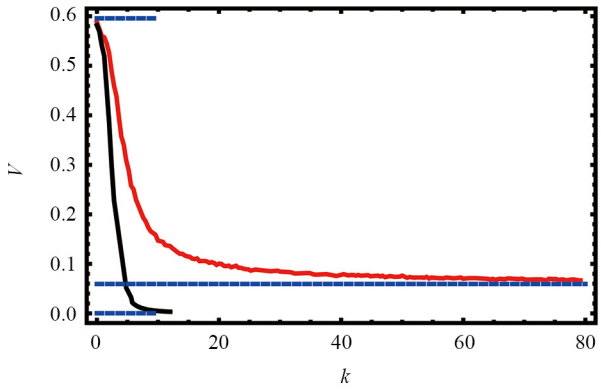

Figure 2. (Color online) The velocity V as a function of k for parameter choice $N = 2$ (red solid line) and $N = 4.0$ (black solid line). In the figure, other parameters are fixed as $N = 2.0$, $f = 0.0$, $U_0 = 6.0$ and $\tau = 2.0$. The blue lines are from the exact analytic results (Equation (8)) both in the limit of $k \to \infty$ and $k \to 0$

Figure 2 plots the velocity V as a function of k for parameter choice $N = 2$ (red solid line) and $N = 4.0$ (black solid line). In the figure, other parameters are fixed as $N = 2.0$, $f = 0.0$, $U_0 = 6.0$ and $\tau = 2.0$. The numerical results exhibit that the chain's mobility decreases as k increases. The same figure also depicts that the velocity of the polymer decreases as N increases. In the limit $k \to \infty$, V goes to the velocity of a rigidly coupled polymer (blue line); when $k \to 0$, V approaches the velocity of a single Brownian particle (blue line).

The external load also dictates the direction of the monomers flow. For large load, current reversal may occur and this indicates that the polymer flows from the cold to the hot reservoirs as shown in Figure 3. The figure depicts that when k increases, V increases and at certain k, the velocity does manifest an optimal peak. As k further increased, the velocity decreases and approach the velocity of compact polymer. On the other hand, the mobility of the chain decreases as N increases. Please note that tuning the elastic constant k is feasible in experimental systems. Ligand binding, ionic conditions, or chemical modifications can modulate stiffness in biopolymers like DNA and proteins.

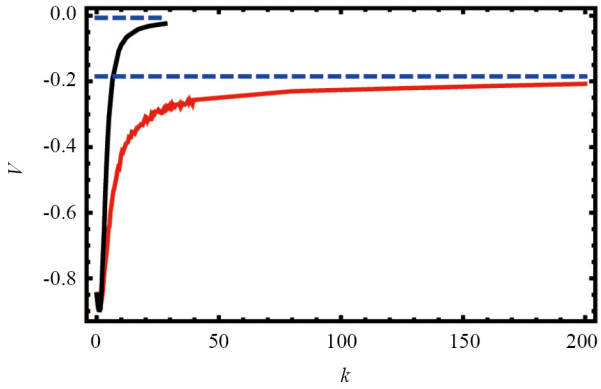

Figure 3. (Color online) The velocity V as a function of k for parameter choice $N = 2$ (red solid line) and $N = 4$ (black solid line). In the figure, other parameters are fixed as $N = 2.0$, $f = 4.0$, $U_0 = 6.0$ and $\tau = 2.0$. The dashed blue lines are from the exact analytic results (Equation (8)) both in the limit of $k \to \infty$ and $k \to 0$

Next via numerical simulations, we explore the dependence of the chain stall force f' on its internal degree of freedoms. Surprisingly the numerical analysis reveals that for the flexible polymers with finite k, the stall force is still independent of N which is in agreement to the exact analytical result for the globular chain (see Equation (9)).

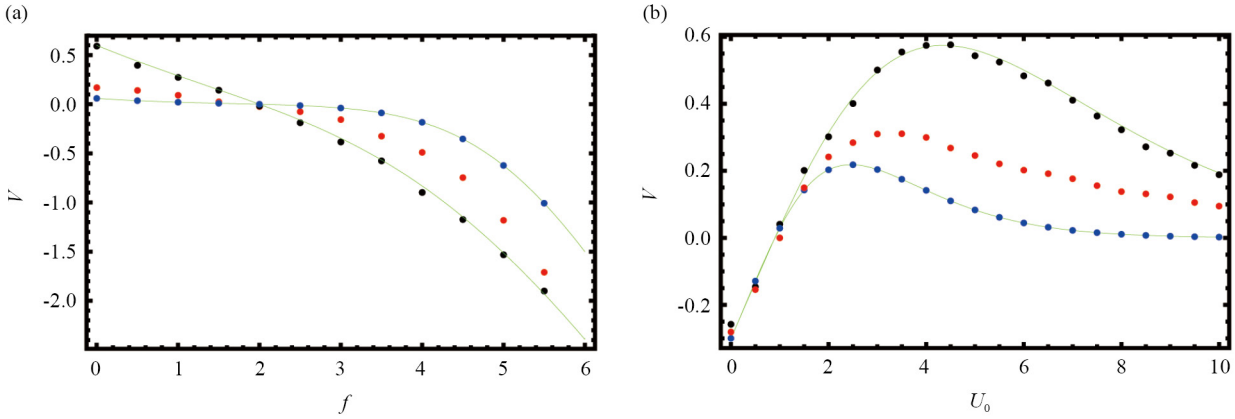

Figure 4. (Color online) (a) The velocity V as a function of f for the parameter values of $U_0 = 6.0$, $N = 2$ and $\tau = 2.0$. The green solid lines stand the plot for V in the limit of $k \to 0$ (top) and $k \to \infty$. The dotted lines are analyzed from the simulations for given values of $k = 0$, $k = 8.0$ and $k = 25.0$ (globular chain) from the top to bottom, respectively. (b) The velocity V as a function of U_0 for parameter choice $k = 0$, $k = 5.0$ and $k = 25.0$ (compact chain), from top to bottom. We also fixed $f = 0.3$, $N = 2$ and $\tau = 2.0$; dotted line stands for the simulation results while green solid lines are form analytic prediction

At this point we want to stress that the external load dictates the direction of the particle flow. When $f < f'$, the net current is positive and while on the contrary for $f > f'$, the current flows from the cold to the hot reservoirs. It worth noting that a larger polymer moves sluggishly than a smaller chain as long as $f \neq f'$. At stall force $f = f'$, the polymer will have zero velocity regardless its size. In Figure 4a, we plot V as a function of f. In the figure, the green solid lines stand the plot for V in the limit of $k \to 0$ (top) and $k \to \infty$. The dotted lines are analyzed from the simulations for given values of $k = 0$, $k = 8.0$ and $k = 25.0$ (globular chain) from the top to bottom, respectively.

As depicted in Figure 4a, for polymer with finite k, current reversal occurs at $f = 2.0$ for parameter choice $U_0 = 6.0$ and $\tau = 2.0$ regardless of the magnitude of k revealing that the coupling strength is not a relevant control parameter to alter the direction of polymers current. On the other hand Figure 4b depicts the plot of V as a function of U_0 for a parameter choice $f = 0.3$ and $\tau = 2.0$. As shown in the figure, the velocity for the polymer monotonously increases with U_0 and attains a maximum value at a particular optimum barrier height U_0^{opt}. Further increasing in U_0 leads to a smaller V. At

U_0^{opt}, the chain retains a maximum speed. The same figure shows that the velocity increases when k decreases. U_0^{opt} also strictly relies on k; when k decreases, U_0^{opt} increases. Furthermore, our analysis exhibits that the transport property of the chain also strictly relies on the temperature difference between the hot and cold baths. When the magnitude of the rescaled temperature τ steps up, the tendency for the polymer in the hot bath to reach the top of the ratchet potential increases than the chain in the cold reservoir. This leads to an increase in the current or velocity.

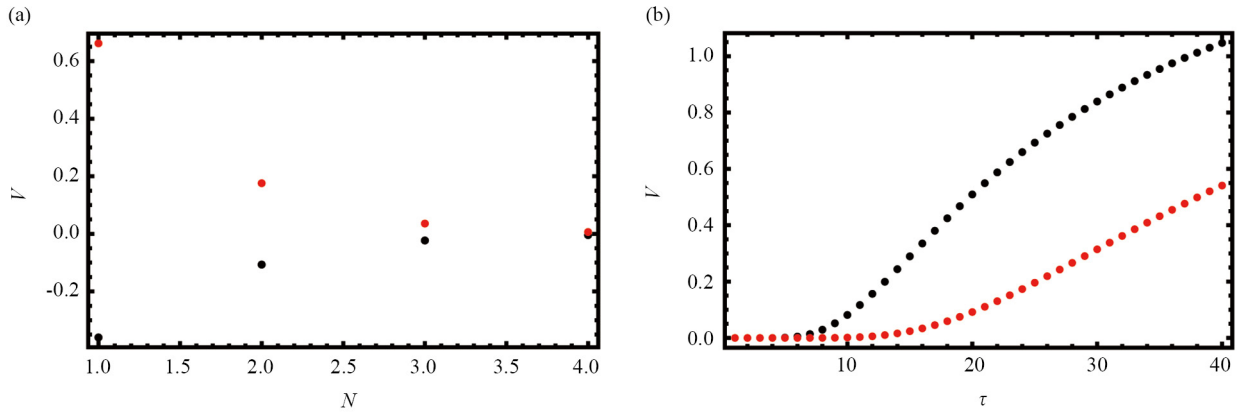

Figure 5. (Color online) (a) The velocity V as a function of N for parameter choice $f = 0$ and $f = 2.0$ from top to bottom. In the figure, other parameters are fixed as $k = 20$, $U_0 = 4.0$ and $\tau = 2.0$. (b) The velocity V as a function of τ for fixed $k = 40$ (compact chain), $U_0 = 4.0$ and $f = 2.0$. The top dotted and the bottom red lines are plotted by taking $N = 8$and $N = 16$, receptively

The dependence of the velocity on chains length is also investigated for parameter choice $f = 0$ and $f = 2.0$ from top to bottom. In the figure, other parameters are fixed as $k = 20$, $U_0 = 4.0$ and $\tau = 2.0$ (see Figure 5a). The figure depicts that when the load is not strong enough, the polymer attains a positive current while for large load, the system exhibits a current reversal. In both cases, the chain velocity monotonously decreases as the chain length decreases. One can note that the peak in velocity versus k is physically intuitive. Moderate coupling allows monomers to move coherently, enhancing directed transport. However, as k increases further, the polymer becomes increasingly rigid and loses flexibility. This limits its ability to adapt to local thermal fluctuations, thereby reducing transport efficiency.

The parameter ranges used in this study are experimentally realistic. Potential barriers of the order of a few k_BT can be implemented using optical traps, structured surfaces, or microfabricated ratchet arrays. Similarly, moderate temperature differences can be established using localized laser heating or thermophoretic gradients. These techniques are widely used in experimental soft matter and microfluidic systems and this makes our model applicable to the practical implementation of polymer transport and sorting.

At this point we want to stress that in this work we explore the behavior of the drift velocity as a function of k and N and showed that the drift velocity is a nontrivial function of these parameters. On the other hand, exploring the transport feature of the chain in terms of the chain length and radius of gyration is vital since these parameters are experimentally relevant parameters. Also exploring the model system in the large N limit is crucial since a reasonable comparison between simulation and experiment can be done only in the large N limit. Next let us investigate qualitatively how the velocity depends on the chain length N and radius of gyration R_G. As discussed in the work [32], the diffusion coefficient $D \propto N^{-r}$ where r is a constant. This clearly shows that the mobility (also velocity shown in Figure 5a) decreases as N decreases. The fact that R_G increases as temperature τ steps up indicates that $D \propto \tau$ which in turn exhibits that the mobility (velocity) increases as the temperature τ steps up (see Figure 5b). All the above results show that the ratio between the chain length L_0 and radius of gyration R_G (R_G/L_0) plays a crucial role. Particularly, since L_0 is fixed, R_G dictates the transport features of the chain.

4. Globular polymer chain

In order gain a deeper insight into this finding, it is instructive to compute the velocity for globular polymer as well as a single Brownian. Simplifying monomer interactions and assuming overdamped dynamics, next we solve the model analytically. Hydrodynamic effects are also neglected and will be addressed in future studies.

In order to rewrite the Langevin equation for compact polymer or rigid polymer ($k \to \infty$) in terms of the center of mass motion, let us add the N Langevin equations [29–31, 33–38] (Equation (3)) to get

$$\frac{d}{dt}\left(\sum_{i=1}^{N} x_i\right) = -\sum_{i=1}^{N} \frac{\partial U(x_i)}{\partial x_i} + \sum_{i=1}^{N} \sqrt{2\gamma T(x_i)}\xi_i(t). \tag{4}$$

When a compact polymer of size N hops on the ratchet potential, each monomer experiences the same force along the reaction coordinate. Hence the effective Langevin equation for the center of mass motion $x_{cm} = (x_1 + x_2 + \ldots x_N)/N$ can be written as

$$N\frac{dx_{cm}}{dt} = -N\frac{\partial U(x_{cm})}{\partial x_{cm}} + \sqrt{2\gamma T(x)}(\xi_1(t) + \ldots + \xi_N(t)). \tag{5}$$

From fluctuation-dissipation relation

$$\langle(\xi_1(t) + \ldots + \xi_N(t))(\xi_1(t) + \ldots + \xi_N(t))\rangle = N\langle\xi(t)^2\rangle \tag{6}$$

which implies that we can substitute $(\xi_1(t) + \ldots + \xi_N(t))$ by $\sqrt{N}\xi(t)$. After some algebra Equation (5) converges to

$$\frac{dx_{cm}}{dt} = -\frac{\partial U(x_{cm})}{\partial x_{cm}} + \sqrt{2\gamma T_{cm}(x)}\xi(t)/\sqrt{N}. \tag{7}$$

The corresponding steady state current J can be exactly evaluated using the same approach as the work [31]. After some algebra, we find a closed form expression for the steady state current

$$J = -\frac{\varsigma_1}{\varsigma_2\varsigma_3 + \varsigma_4\varsigma_1} \tag{8}$$

where the expressions for ς_1, ς_2, ς_3 and ς_4 are given as $\varsigma_1 = e^{a-b} - 1$, $\varsigma_2 = \frac{N}{a\tau}(1-e^{-a}) + \frac{N}{b}e^{-a}\left(e^b - 1\right)$, $\varsigma_3 = \frac{1}{a}(e^a - 1) + \frac{1}{b}e^a\left(1 - e^{-b}\right)$. The parameter ς_4 is given by $\varsigma_4 = \varepsilon_1 + \varepsilon_2 + \varepsilon_3$ where $\varepsilon_1 = \frac{N}{\tau}\left(\frac{1}{a}\right)^2(a + e^{-a} - 1)$, $\varepsilon_2 = \frac{N}{ab}(1-e^{-a})\left(e^b - 1\right)$, $\varepsilon_3 = N\left(\frac{1}{b}\right)^2\left(e^b - 1 - b\right)$. Here $a = N(U_0 + f)/\tau$ and $b = N(U_0 - f)$. The corresponding velocity is given by $V = 2J$. In the limit $f \gg U_0$ and large N we have $a \approx Nf/\tau$, $b \approx -Nf$, $\varsigma_1 \approx \exp[Nf/\tau + Nf]$, $\varsigma_2 \approx 1/f$, $\varsigma_3 \approx \exp[(Nf/\tau + Nf)]/Nf$, $\varepsilon_1 \approx 1/f$, $\varepsilon_2 \approx 0$ and $\varepsilon_3 \approx 1/f$. Substituting these values, we get $J \approx -f/2$.

Moreover, the exact analytical result for the globular chain uncovers that the stall force

$$f' = \frac{U_0(\tau-1)}{(\tau+1)} \tag{9}$$

at which the chain current vanishes, is independent of the chain length N. The stall force in our model is remarkably independent of both the chain length and coupling strength. This contrasts with earlier studies where stall force typically scaled with polymer size or stiffness. Our results highlight a unique symmetry in the center-of-mass dynamics under thermal gradients. This offers a practical advantage for polymer sorting by allowing size-independent control using a single external force.

In the absence of external load $f = 0$, the steady state current (Equation (8)) converges to

$$J = \frac{NU_0^2}{2(1+\tau)}\left[\frac{1}{e^{\frac{NU_0}{\tau}}-1} - \frac{1}{e^{NU_0}-1}\right]. \tag{10}$$

For small U_0, it is straight forward to show $J \approx \frac{U_0}{2}\left(\frac{\tau-1}{\tau+1}\right)$. On the other hand for large U_0 and τ, one approximates Equation (10) as $J \approx \frac{NU_0^2}{2(1+\tau)} e^{\frac{-NU_0}{\tau}}$. The current J and the velocity align with the established scaling laws in polymer dynamics, where the diffusion coefficient scales as $D \sim N^{-\nu}$, with $\nu \approx 1$ for one-dimensional Rouse-like behavior. In our simulations, the drift velocity decreases monotonically with increasing chain length N, reflecting the reduced mobility for longer polymers. The effective scaling exponent extracted from the velocity vs. N plots closely matches the theoretical prediction for the 1 D Brownian motion of flexible chains. This agreement confirms that our model correctly captures the key features of size-dependent transport in overdamped regimes.

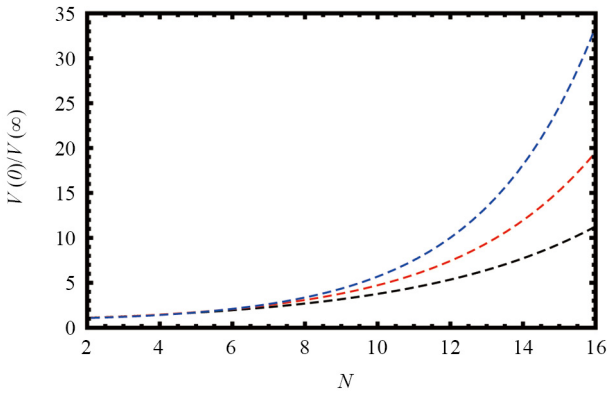

Figure 6. The ratio $V(k \to 0)/V(k \to \infty)$ as a function of N for parameter choice $f = 0.0$ (black solid line), $f = 0.5$ (red solid line), $f = 1.0$ (blue solid line). Other parameters are fixed as $U_0 = 2.0$ and $\tau = 8.0$

Closer look at the Figure 2 once again reveals that the chain retains a higher velocity $V(0)$ at $k = 0$ than the velocity $V(\infty)$ of a globular chain ($k \to \infty$). Particularly, as the size of the chain increases, the gap between $V(0)$ and $V(\infty)$ increases. To analyze the chain size dependence further, we have computed the ratio for the velocity of a single particle to globular polymer utilizing Equation (8). As exhibited in Figure 6, V is a nontrivial function of N; the polymer with small k retains considerably higher velocity than a rigid dimer. This signifies that attenuating the strength of the elastic constant results in a polymer that can be transported fast. The ratio $V(k \to 0)/V(k \to \infty)$ quantifies the enhancement in transport due to polymer flexibility. A higher ratio indicates that a flexible chain moves significantly faster than a rigid one under the same

external conditions. This metric provides a practical means of assessing how elastic properties affect mobility, which can inform the design of polymer-based transport systems or sorting devices. However, it also has limitations since it does not account for other realistic factors such as hydrodynamic interactions, crowding effects, or non-linear stiffness in long chains. This can be notably appreciated by taking the velocity ratio between a single and globular polymer in high barrier limit which is given as

$$\frac{V(0)}{V(\infty)} = \frac{e^{\frac{(-1+N)(fL_0+U_0)}{\tau}}}{N} \tag{11}$$

where in the limit $f \to 0$, $\frac{V(0)}{V(\infty)} = \frac{\exp^{\frac{(-1+N)(U_0)}{\tau}}}{N}$. This can be retrieved using our previous calculations since for large U_0, $J \approx \frac{NU_0^2}{2(1+\tau)} e^{\frac{-NU_0}{\tau}}$.

The central results of this paper also indicates the occurrence a direct relationship between the flexibility of a macromolecule and its transport properties. Hence, we expect that in general this relationship can be applied to control the transport of molecules by modulating their flexibility. Modifying the flexibility of a macromolecule can be achieved in a variety of ways. Experimentally, the flexibility of the chain can be manipulated in a variety of ways. For instance, the flexibility of proteins can be altered by ligand binding [39]. The elasticity of the DNA molecule can be also strengthen by introducing external charges [40]. Thermal and chemical denaturation also alter the flexibility of biological molecules since hydrogen bond breaking leads to an increase in the rotational degrees of freedom of atoms and thereby increases the macroscopic flexibility of the molecule [41, 42].

5. Summary and conclusion

In this study, we have systematically examined the transport and response properties of a single flexible polymer moving in a ratchet potential under the influence of an external load. The surrounding viscous medium is alternately in contact with spatially varying thermal reservoirs along the reaction coordinate, driving the system far from equilibrium. Our findings reveal that each monomer of the chain exhibits a fast unidirectional current, with the strength of current rectification depending not only on thermal fluctuations and external loading but also on the chain's coupling strength and size in a nontrivial manner.

Our numerical and exact analytical results demonstrate that the stall force, at which the net current of the polymer vanishes, is independent of both the chain length N and the coupling strength k. Additionally, we show that a more flexible polymer attains a higher velocity compared to a stiffer chain, indicating that transport properties can be effectively tuned by modulating the elastic coupling strength. This result suggests a novel mechanism for designing polymers with targeted transport speeds by attenuating the elastic constant, which can be achieved experimentally through ligand binding [39], the introduction of external charges [40], or chemical denaturation [41, 42].

Beyond providing insight into the fundamental transport mechanisms of polymers in ratchet potentials, our findings have potential applications in nanoscale transport and biomolecular sorting. The ability to control polymer mobility by tuning system parameters opens avenues for optimizing directed transport in synthetic and biological systems. Future work may explore the impact of additional interactions, such as hydrodynamic effects or external field modulations, on the rectified motion of flexible polymers, further expanding the applicability of these findings to engineered nanoscale devices.

In conclusion, in this work, we present a pragmatic model system which not only serves as a basic guide on how to transport the polymer fast to specific region but also has novel applications for binding kinetics, DNA amplifications and sorting of multicomponent systems based on their dominant parameters.

Acknowledgement

I would like also to thank Mulu Zebene for the constant support.

Conflict of interest

The author declares no competing financial interest.

References

[1] Hänggi P, Talkner P, Borkovec M. Reaction-rate theory: Fifty years after Kramers. *Reviews of Modern Physics*. 1990; 62: 251. Available from: https://doi.org/10.1103/RevModPhys.62.251.

[2] Sebastian KL, Debnath A. Polymer in a double well: Dynamics of translocation of short chains over a barrier. *Journal of Physics: Condensed Matter*. 2006; 18: S283. Available from: https://doi.org/10.1088/0953-8984/18/14/S12.

[3] Park PJ, Sung W. Dynamics of a polymer surmounting a potential barrier: The Kramers problem for polymers. *Journal of Chemical Physics*. 1999; 111(11): 5259-5266. Available from: https://doi.org/10.1063/1.479779.

[4] Lee S, Sung W. Coil-to-stretch transition, kink formation, and efficient barrier crossing of a flexible chain. *Physical Review E*. 2001; 63(2): 021115. Available from: https://doi.org/10.1103/PhysRevE.63.021115.

[5] Marchesoni F, Cattuto C, Costantini G. Elastic strings in solids: Thermal nucleation. *Physical Review B*. 1998; 57(13): 7930-7934. Available from: https://doi.org/10.1103/PhysRevB.57.7930.

[6] Sebastian KL, Paul AKR. Kramers problem for a polymer in a double well. *Physical Review E*. 2000; 62(1): 927-931. Available from: https://doi.org/10.1103/PhysRevE.62.927.

[7] Lindner JF, Meadows BK, Ditto WL, Inchiosa ME, Bulsara AR. Array enhanced stochastic resonance and spatiotemporal synchronization. *Physical Review Letters*. 1995; 75(1): 3-6. Available from: https://doi.org/10.1103/PhysRevLett.75.3.

[8] Marchesoni F, Gammaitoni L, Bulsara AR. Spatiotemporal stochastic resonance in a ϕ^4 model of kink-antikink nucleation. *Physical Review Letters*. 1996; 76(15): 2609-2612. Available from: https://doi.org/10.1103/PhysRevLett.76.2609.

[9] Dikshtein IE, Kuznetsov DV, Schimansky-Geier L. Stochastic resonance for motion of flexible macromolecules in solution. *Physical Review E*. 2002; 65(6): 061109. Available from: https://doi.org/10.1103/PhysRevE.65.061101.

[10] Asfaw M, Sung W. Stochastic resonance of a flexible chain crossing over a barrier. *Europhysics Letters*. 2010; 90(3): 30008. Available from: https://doi.org/10.1209/0295-5075/90/30008.

[11] Asfaw M. Thermally activated barrier crossing and stochastic resonance of a flexible polymer chain in a piecewise linear bistable potential. *Physical Review E*. 2010; 82(2): 021111. Available from: https://doi.org/10.1103/PhysRevE.82.021111.

[12] Asfaw M, Shiferaw Y. Exploring the dynamics of dimer crossing over a Kramers type potential. *Journal of Chemical Physics*. 2012; 136(2): 025101. Available from: https://doi.org/10.1063/1.3675920.

[13] Jung P, Behn U, Pantazelou E, Moss F. Collective response in globally coupled bistable systems. *Physical Review A*. 1992; 46(3): R1709. Available from: https://doi.org/10.1103/PhysRevA.46.R1709.

[14] Pototsky A, Marchesoni F, Savel'ev SE. Ratcheting of neutral elastic dimers on a charged filament. *Physical Review E*. 2010; 81(3): 031114. Available from: https://doi.org/10.1103/PhysRevE.81.031114.

[15] Pototsky A, Janson NB, Marchesoni F, Savel'ev SE. Directed transport in periodically rocked random ratchets. *Chemical Physics*. 2010; 375(2-3): 458-464. Available from: https://doi.org/10.1103/PhysRevE.79.051102.

[16] Heinsalu E, Patriarca M, Marchesoni F. Dimer diffusion in a washboard potential. *Physical Review E*. 2008; 77(2): 021129. Available from: https://doi.org/10.1103/PhysRevE.77.021129.

[17] Braun OM, Ferrando R, Tommei GE. Stimulated diffusion of an adsorbed dimer. *Physical Review E*. 2003; 68(5): 051101. Available from: https://doi.org/10.1103/PhysRevE.68.051101.

[18] Fusco C, Fasolino A, Janssen T. Nonlinear dynamics of dimers on periodic substrates. *European Physical Journal B*. 2003; 31(1): 95-101. Available from: https://doi.org/10.1140/epjb/e2003-00013-y.

[19] Burada PS, Schmid G, Reguera D, Vainstein MH, Rubi JM, Hänggi P. Entropic stochastic resonance: The constructive role of the unevenness. *Physical Review Letters*. 2008; 101(13): 130602. Available from: https://doi.org/10.1140/epjb/e2009-00051-5.

[20] Benzi R, Parisi G, Sutera A, Vulpiani A. Stochastic resonance in climatic change. *Tellus*. 1982; 34(1): 10-16. Available from: https://doi.org/10.3402/tellusa.v34i1.10782.

[21] Gammaitoni L, Hänggi P, Jung P, Marchesoni F. Stochastic resonance. *Reviews of Modern Physics*. 1998; 70(1): 223-287. Available from: https://doi.org/10.1103/RevModPhys.70.223.

[22] Klumpp S, Mielke A, Wald C. Noise-induced transport of two coupled particles. *Physical Review E*. 2000; 63: 031914. Available from: https://doi.org/10.1103/PhysRevE.63.031914.

[23] Downton MT, Zuckermann MJ, Craig EM, Plischke M, Linke H. Single-polymer Brownian motor: A simulation study. *Physical Review E*. 2006; 73: 011909. Available from: https://doi.org/10.1103/PhysRevE.73.011909.

[24] Polson JM, Bylhouwer B, Zuckermann MJ, Horton AJ, Scott WM. Dynamics of a polymer in a Brownian ratchet. *Physical Review E*. 2010; 82: 051931. Available from: https://doi.org/10.1103/PhysRevE.82.051931.

[25] Kalhori A, Bayat MJ, Asemi K. Buckling analysis of stiffened functionally graded multilayer graphene platelet. *Results in Engineering*. 2023; 20: 101563. Available from: https://doi.org/10.1016/j.rineng.2023.101563.

[26] Cho JR. Buckling analysis of functionally graded GPL-reinforced composite plates under combined thermal and mechanical loads. *Materials*. 2025; 18(3): 567. Available from: https://doi.org/10.3390/ma18030567.

[27] Gao XY, Wang ZZ, Ma LS. Bending and buckling analysis of functionally graded graphene platelets reinforced composite plates supported by local elastic foundations based on simple refined plate theory. *Archive of Applied Mechanics*. 2024; 94: 2123-2150. Available from: https://doi.org/10.1007/s00419-024-02629-y.

[28] Roun S, Nguyen VL, Rungamornrat J. Free vibration and buckling analyses of functionally graded plates with graphene platelets reinforcement. *ASME Journal of Computing and Information Science in Engineering*. 2025; 25: 011002. Available from: https://doi.org/10.1115/1.4064665.

[29] Büttiker M. Transport as a consequence of state-dependent diffusion. *Zeitschrift für Physik B*. 1987; 68: 161-167. Available from: https://doi.org/10.1007/BF01304221.

[30] Van Kampen NG. Diffusion in inhomogeneous media. *Journal of Physics and Chemistry of Solids*. 1988; 49(6): 673-677. Available from: https://doi.org/10.1016/0022-3697(88)90199-0.

[31] Asfaw M, Bekele M. Current, maximum power and optimized efficiency of a Brownian heat engine. *European Physical Journal B*. 2004; 38: 457-461. Available from: https://doi.org/10.1140/epjb/e2004-00140-y.

[32] Desai TG, Keblinski P, Kumar SK, Granick S. Molecular-dynamics simulations of the transport properties of a single polymer chain in two dimensions. *Journal of Chemical Physics*. 2006; 124(8): 084904. Available from: https://doi.org/10.1063/1.2161197.

[33] Asfaw M. Modeling an efficient Brownian heat engine. *European Physical Journal B*. 2008; 65: 109-116. Available from: https://doi.org/10.1140/epjb/e2008-00308-5.

[34] Landauer R. Motion out of noisy states. *Journal of Statistical Physics*. 1988; 53: 233-248. Available from: https://doi.org/10.1007/BF01011555.

[35] Landauer R. Inadequacy of entropy and entropy derivatives in characterizing the steady state. *Physical Review A*. 1975; 12: 636. Available from: https://doi.org/10.1103/PhysRevA.12.636.

[36] Büttiker M, Landauer R. Thermally activated escape from underdamped metastable wells. *Physical Review Letters*. 1984; 52(14): 1250-1253. Available from: https://doi.org/10.1103/PhysRevLett.52.1250.

[37] Matsuo M, Sasa S. Stochastic energetics of non-uniform temperature systems. *Physica A: Statistical Mechanics and its Applications*. 1999; 276(1-2): 188-200. Available from: https://doi.org/10.1016/S0378-4371(99)00365-9.

[38] Jülicher F, Ajdari A, Prost J. Modeling molecular motors. *Reviews of Modern Physics*. 1997; 69: 1269. Available from: https://doi.org/10.1103/RevModPhys.69.1269.

[39] Najmanovich RL, Kuttner J, Sobolev V, Edelman M. Side-chain flexibility in proteins upon ligand binding. *Proteins*. 2000; 39: 261-268. Available from: https://doi.org/10.1002/(sici)1097-0134(20000515)39:3<261::aid-prot90>3.0.co;2-4.

[40] Podest A, Indrieri M, Brogioli D, Manning GS, Milani P, Guerra R, et al. Positively charged surfaces increase the flexibility of DNA. *Biophysical Journal*. 2005; 89(4): 2558-2563. Available from: https://doi.org/10.1529/biophysj.105.064667.

[41] Schulze B, Sljoka A. Protein flexibility of dimers: Do symmetric motions play a role in allosteric interactions? *AIP Conference Proceedings*. 2011; 1368: 135-138. Available from: https://doi.org/10.1063/1.3663478.

[42] Rader AJ, Hespenhelde BM, Kuhn LA, Thorpe MF. Protein Unfolding: Rigidity Lost. *Proceedings of the National Academy of Sciences of the United States of America*. 2002; 99(6): 3540-3545 Available from: https://doi.org/10.1073/pnas.062492699.